Published in final edited form as:
J Comp Neurol. 2014 April 1; 522(5): 1191–1208. doi:10.1002/cne.23497.

Specificity and efficiency of reporter expression in adult neural progenitors varies substantially among nestin-CreER^{T2} lines

Min-Yu Sun[1], **Michael J. Yetman**[1], **Tang-Cheng Lee**[1], **Yuqing Chen**[2], and **Joanna L. Jankowsky**[1,3,4]

[1]Department of Neuroscience, Baylor College of Medicine, Houston, TX

[2]Department of Human and Molecular Genetics, Baylor College of Medicine, Houston, TX

[3]Department of Neurology, and Neurosurgery, Baylor College of Medicine, Houston, TX

[4]Huffington Center on Aging, Baylor College of Medicine, Houston, TX

Abstract

Transgenic lines expressing a controllable form of Cre recombinase have become valuable tools for manipulating gene expression in adult neural progenitors and their progeny. Neural progenitors express several proteins that distinguish them from mature neurons and the promoters for these genes have been co-opted to produce selective transgene expression within this population. To date, nine CreER^{T2} transgenic lines have been designed using the *nestin* promoter, however, only a subset are capable of eliciting expression within both neurogenic zones of the adult brain. Here we compare three such nestin-CreER^{T2} lines to evaluate specificity of expression and efficiency of recombination. Each line was examined using three different Cre reporter strains that varied in sensitivity. We found that all three nestin-CreER^{T2} strains induced reporter expression within the main neurogenic areas, albeit to varying degrees depending on the reporter. Unexpectedly, we found that two of the three lines induced substantial reporter expression outside of neurogenic areas. These lines produced strong labeling in cerebellar granule neurons, with additional expression in cortex, hippocampus, striatum, and thalamus. Reporter expression in the third nestin-CreER^{T2} line was considerably more specific, but was also less efficient, labeling a smaller percentage of the target population than the other two drivers. Our findings suggest that each nestin-CreER^{T2} line may best serve different experimental needs, depending on whether specificity or efficiency is of greatest concern. Our study further demonstrates that each new pair of driver and responder lines should be evaluated independently, as both components can significantly influence the resulting expression pattern.

Keywords

Adult hippocampal neurogenesis; subgranular zone; ectopic expression; lineage tracing; cerebellum; ROSA26 Cre reporter

Correspondence to: Joanna L. Jankowsky, Baylor College of Medicine, BCM295, One Baylor Plaza, Houston, TX 77030; jankowsk@bcm.edu.

Conflict of Interest
The authors declare no conflict of interest.

Introduction

The function of adult-born neurons has been intensively studied since their rediscovery in the early 1990's (reviewed in (Gould, 2007)). New neurons generated in sub-ventricular zone (SVZ) of the lateral ventricle migrate through the rostral migratory stream to become granule cells and interneurons of the olfactory bulb, while those born in the sub-granular zone (SGZ) of the dentate gyrus move into the neighboring granule cell layer to become granule cells of the hippocampus (DGCs). During their maturation, adult-born neurons in the hippocampus undergo a period of heightened plasticity that transiently distinguishes them from neighboring mature neurons (reviewed in (Ming and Song, 2011)). This temporary period of enhanced plasticity may facilitate differentiation of new experiences from old by activating distinct sets of neurons within the dentate at each time (reviewed in (Aimone et al., 2011; Aimone et al., 2006; Deng et al., 2010)). A complementary hypothesis holds that adult-born DGCs play a key role in pattern separation by allowing an unending supply of new neurons to enlist for information storage (reviewed in(Sahay et al., 2011b; Yassa and Stark, 2011)). In contrast to these primarily cognitive-enhancing roles proposed for adult neurogenesis in the dorsal hippocampus, newborn DGCs in the ventral hippocampus are thought to modulate the response to stress and mediate the effects of certain anti-depressant medications (reviewed in (Eisch and Petrik, 2012; Petrik et al., 2012). Whether they regulate memory in the dorsal hippocampus or mood in the ventral, this small population of specialized neurons is uniquely positioned to affect brain function as a whole (reviewed in (Snyder and Cameron, 2012)).

Experimentally testing hypotheses about the function of adult-born neurons requires a means of specifically manipulating these cells in vivo. Past studies have used their proliferative potential as a vulnerability that can be exploited to ablate the dividing progenitors with x-ray irradiation or antimitotic agents so that behavior can be tested in their absence (reviewed in (Marin-Burgin and Schinder, 2012)). More recent studies have used genetic approaches to identify and either eliminate or enhance the function of progenitors and their progeny (Arruda-Carvalho et al., 2011; Imayoshi et al., 2008; Niibori et al., 2012; Sahay et al., 2011a). Unlike embryonic-born mature neurons, adult NPCs retain markers of multipotency such as *nestin* and *Sox2* that can be used to selectively access them with genetic tools (reviewed in (Imayoshi et al., 2011)). By combining spatial specificity of the *nestin* promoter with genetic elements such as CreER^{T2} that provide temporal control over their activity, multiple groups have created transgenic mouse lines that allow selective manipulation of adult neural progenitor cells without affecting their embryonic-born neighbors (reviewed in (Imayoshi et al., 2011), also see (Dranovsky et al., 2011)).

The value of these new transgenic tools is in their assumed specificity for adult-born neurons, yet several groups have reported gene expression in areas outside the expected neurogenic regions (Alcantara Llaguno et al., 2009; Chen et al., 2009). In addition to the SGZ and SVZ, Parada and colleagues observed prominent neuronal labeling in the granular layer of the cerebellum following tamoxifen treatment of their nestin-CreER^{T2} animals (Alcantara Llaguno et al., 2009; Chen et al., 2009). Such ectopic ‘leak’ could significantly impact the interpretation of behavioral experiments using these lines. In the present study, we set out to compare the efficiency and specificity of recombination in three nestin-

CreER^{T2} lines reported to drive expression in the hippocampal SGZ. By crossing each driver with three distinct ROSA26-targeted reporter lines, we provide a side-by-side comparison of Cre-induced gene expression among the resulting bigenic mice. Our results demonstrate that expression in these systems is influenced by both the strength of the driver and the stringency of the responder. While our findings offer a starting point for others to use in selecting lines for study, they also underline the need for careful assessment of each new driver-responder pair to ensure that the expected genetic manipulation is actually attained.

Materials and Methods

Transgenic lines

Six strains of transgenic mice were used in this study. The three nestin-CreER^{T2} driver lines were kind gifts of Amelia Eisch (line K, congenic C57BL/6 background; now available from The Jackson Laboratories as stock #16261 (Lagace et al., 2007)), Rene Hen (here referred to as line H, hybrid B6129 background; (Dranovsky et al., 2011)), and Ryoichiro Kageyama (line 4, congenic C57BL/6 background; (Imayoshi et al., 2006)). To test Cre recombination efficiency, these driver lines were each mated with three ROSA26-targeted responder lines: Ai3 CAG-lox-stop-lox-eYFP on a congenic C57BL/6J background (Jackson Laboratories stock #7903 (Madisen et al., 2010)), R26R lox-stop-lox-lacZ on a congenic C57BL/6J background (Jackson Laboratories stock #3474 (Soriano, 1999)) and GluCl CAG-lox-stop-lox-GluClα-2A-GluClβ-2A-YFP on a congenic C57BL/6J background (described briefly below, but used here only as a more stringent YFP Cre reporter than Ai3). The resulting double-transgenic strains were: 1) nestin-CreER^{T2} line K × Ai3, 2) nestin-CreER^{T2} line K × R26R-lacZ, 3) nestin-CreER^{T2} line K × GluCl, 4) nestin-CreER^{T2} line H × Ai3, 5) nestin-CreER^{T2} line H × R26R-lacZ, 6) nestin-CreER^{T2} line H × GluCl, 7) nestin-CreER^{T2} line 4 × Ai3, 8) nestin-CreER^{T2} line 4 × R26R-lacZ, and 9) nestin-CreER^{T2} line 4 × GluCl. Breeder cages were maintained on high-fat chow (Purina PicoLab mouse diet 20, #5058). Offspring were moved to standard chow at weaning and remained on this diet until harvest (LabDiet Laboratory rodent diet #5001). Bigenic offspring were verified by tail biopsy before the onset of experiments. Two to five mice from each genotype were assessed with and without tamoxifen induction. Both male and female offspring were used for analysis. All procedures were reviewed and approved by the Baylor College of Medicine Institutional Animal Care and Use Committee in accordance with the guidelines of the U.S. National Institutes of Health.

Construction of the Cre-dependent GluCl^{YFP} reporter line

We generated a transgenic mouse to express a codon-optimized variant of the *C. elegans* glutamate-gated chloride channel (GluCl)(Slimko and Lester, 2003). The transgene contained the coding sequences of both α and β subunits of the GluCl channel along with enhanced YFP as a vital label for expression. Coding sequences for GluClα and GluClβ were amplified from pAAV2-GluClα-CFP and pAAV2-GluClβY182F-YFP respectively (Lerchner et al., 2007). Fluorescent CFP and YFP labels that had been fused into the intracellular domains of the original constructs were removed during cloning. YFP was amplified from pEYFP-N1 (Clontech). The GluClα, GluClβ, and YFP coding sequences

were separated in-frame by addition of *Thosea asigna* virus TaV 2A sequences during PCR amplificaiton, allowing equimolar expression of the three proteins (GGCAGTGGAGAGGGCAGAGGAAGTCTGCTAACATGCGGTGACGTCGAGGAGA ATCCTGGCCCA)(Trichas et al., 2008). The tripartite open reading frame was cloned into NheI/XhoI sites of the ROSA26-targeting helper plasmid pBigT (Srinivas et al., 2001). Rather than rely on the weak expression provided by the endogenous ROSA26 promoter, we cloned the CMV early enhancer/chicken β-actin (CAG) promoter from pCAG-GFP-WPRE (Zhao et al., 2006) by digestion with SalI and NheI and ligated it into the SalI/AvrII sites of pBigT. Transgene expression was regulated by insertion of the loxP-flanked stop cassette contained within pBigT. The woodchuck hepatitis virus posttranscriptional regulatory element (WPRE) was amplified from pAAV2-GluCl α-WPRE (Lerchner et al., 2007) and cloned into the XhoI/NotI sites of pBigT. The complete CAG-loxP-stop-loxP-GluClα-GluClβ-eYFP-WPRE construct was then digested with PacI and AscI and cloned into the targeting vector pROSA26PA(Srinivas et al., 2001) which had previously been modified with a linker between the Xho1 and Kpn1 sites to add the unique restriction sites Mlu1, Fse1, and AsiS1 for later linearization of the targeting vector. pROSA26PA containing the CAG-loxP-stop-loxP-GluClα-GluClβ-eYFP-WPRE insert was linearized with MluI, purified, and electroporated into agouti C57BL/6N JM8 embryonic stem cells (Pettitt et al., 2009). Clones were screened by Southern blotting with a probe specific for the 5' targeting arm for correct insertion. Two clones were amplified and injected into C57BL/6 albino blastocysts, yielding 20 offspring, of which one male was used to found the line described here. The line was subsequently maintained by backcross onto C57BL/6J.

Tamoxifen treatment

Tamoxifen solution (30 mg/ml) was prepared by dissolving tamoxifen (Sigma T5648) in a mix of 10% ethanol (Aaper, 200 proof # E200) and 90% sunflower seed oil (Sigma S5007). Starting at 8 weeks of age, mice were treated with 5 daily injections of tamoxifen solution at a dose of 180 mg/kg i.p., followed by a 7 day recovery prior to harvest. Control groups were administered the same dose of vehicle (ethanol and sunflower seed oil) without tamoxifen. Tamoxifen solution was made fresh prior to the first injection of each animal and was stored at 4 °C for no more than one week.

Tissue preparation

Fluorescent reporter lines—Mice were sacrificed by carbon dioxide inhalation 7 days after the final injection of either tamoxifen or vehicle. Brains were immersion fixed for 24 hours at 4° C in fresh 4% paraformaldehyde (PFA) and then transferred to 30% sucrose in phosphate-buffered saline (PBS) for cryoprotection.

β-galactosidase reporter lines—Seven days after the final injection of either tamoxifen or vehicle, mice were anaesthetized by i.p. injection of pentobarbital and transcardially perfused with ice-cold PBS containing 10 U/ml heparin followed by 4% PFA. Brains were harvested and post-fixed by immersion in 4% PFA at 4° C for 3 hours, and then transferred to 30% sucrose in PBS at 4°C for cryoprotection.

All tissue—Following equilibration in sucrose, tissue was frozen on dry ice for cryosectioning. Horizontal sections were made at 40 μm using a freezing-sliding microtome. Sections were stored in antifreeze solution [50 mM $NaPO_4$, pH 7.4, containing 25% glycerol and 30% ethylene glycol (v/v)] at −20 °C until use.

Ai3 reporter lines—Sections from nestin-CreER^{T2} × Ai3 lines were mounted directly onto slides (Fisher Superfrost Plus) to assess native YFP expression.

Antibody characterization

Calbindin D-28k was detected with a rabbit polyclonal raised against recombinant full-length rat calbindin D-28k. According to the manufacturer's information sheet, the antibody detects a single band at 27-28 kD on immunoblots of brain homogenate from a variety of vertebrate animals, but will cross-react with calretinin under non-native conditions where calretinin levels reach more than 10-fold those of calbindin. The manufacturer also reports that the antibody detects a subpopulation of neurons in the healthy mouse brain, but shows no specific labeling in mice null for calbindin. In our tissue, calbindin staining with this antibody was used to identify medium spiny neurons, as previously characterized by Huang et al. (Huang et al., 1995)

Collagen type IV was detected with a rabbit polyclonal raised against full-length collagen IV purified from human and cow placenta. According to the manufacturer's information sheet, the antibody detects a single band of 200 kD by Western blot of mouse muscle lysate, and has negligible cross-reactivity with other collagen types I, II, III, V, or VI. Immunostaining with this antibody labeled the basal lamina of blood vessels within the brain, consistent with the staining pattern expected for this antigen (Urabe et al., 2002).

YFP was detected with a chicken polyclonal antibody raised against the recombinant full-length synthetic green fluorescent protein of *Aequorea victoria* (Table 1). According to the manufactuer's information sheet, the antibody detects both GFP and all of its spectral variants including YFP. The antibody detects a single band at 27-30 kD on Western blot from mouse spinal cord extract in transgenic lines expressing GFP and in cell lines transfected with GFP vector (Abcam data sheet). Immunostaining of non-transgenic brain sections with this antibody shows no detectable staining.

Nestin was detected with a mouse monoclonal antibody raised against full-length nestin protein purified from embryonic rat spinal cord (Hockfield and McKay, 1985). According to the manufacter's information sheet, antibody specificity has been confirmed in mouse and rat tissue, where it recognizes a band of 200-220 kD. This antibody has been used to detect neural progenitor cells in numerous studies cited by the manufacturer. Consistent with the published literature, cells in the SGZ and SVZ with the morphology of neural progenitors stained positive for nestin in our tissue.

Parvalbumin was detected with a goat polyclonal antibody raised against endogenous protein purified from rat muscle. According to the manufacturer's information sheet, the antibody detects a single band at approximately 12 kD (monomer) in brain homogenates from 5 out of 7 vertebrate species tested, with an additional band at 24 kD (dimer) in mice

and rats. The information sheet demonstrates specific labeling of GABAergic interneurons in the mouse cortex that is absent from parvalbumin null mice. In our tissue, this antibody detected interneurons within the molecular layer of the cerebellum, consistent with published reports of parvalbumin labeling in basket and stellate cells of the mouse cerebellum (Schwaller et al., 2002).

S100 calcium binding protein B was detected with a rabbit polyclonal antibody raised against full-length S100 protein purified from cow brain. According to the manufacturer's information sheet, the antibody detects a doublet of S100 proteins on crossed immunoelectrophoresis of both cow and human brain extracts, and on Western blot of recombinant proteins reacts most strongly with S100B, weakly with S100A1 and A6, and does not detect S100A2, A3, or A4. In our tissue, the antibody stained cells with the morphology and distribution of astrocytes, consistent with past reports for this protein, where labeling in healthy human cortex was primarily astrocytic (Steiner et al., 2007)

Immunohistochemistry

All sections were rinsed with Tris-buffered saline (TBS) to remove residual antifreeze solution before use.

YFP, Parvalbumin, calbindin, S100B, and collagen IV—Sections from nestin-CreER^{T2} × GluCl lines, were immunostained for YFP to enhance the fluorescent signal. Sections from nestinCreER^{T2} × Ai3 lines were immunostained for parvalbumin to identify cerebellar and cortical interneurons, calbindin to identify striatal medium spiny neurons and cortical interneurons, S100B to identify astrocytes, and collagen IV to identify vascular endothelial cells. Sections were blocked for 1 hour at room temperature (5% goat serum, 1% BSA, 0.5% Tween- 20 and 0.1% Triton-X 100 in TBS) and then incubated overnight at 4° C with primary antibody diluted in blocking solution. The following day, sections were rinsed with TBS and incubated with Alexa Fluor 488-conjugated (YFP only) or Alexa Fluor 568-conjugated secondary antibody diluted 1:500 in blocking solution for 2 hours at room temperature (Invitrogen, anti-chicken A11039, anti-goat A11057, anti-rabbit A11011). Sections were mounted with aqueous anti-fade mounting medium (Vectashield H-1400, Vector Laboratories) and processed for fluorescent detection.

YFP and nestin co-immunostain—A subset of sections from nestin-CreER^{T2} × GluCl lines were immunostained for both YFP and nestin. Antigen retrieval was performed by incubating sections in 10 mM sodium citrate, pH 6.0 at 80° C for 25 min. Sections were allowed to cool to room temperature during three 10 min rinses in TBS, before being processed for YFP and nestin immunofluorescence as described above, followed by detection with Alexa Fluor conjugated secondary antibodies diluted 1:500 in block (Invitrogen, anti-chicken A11039 and anti-mouse A21124).

βμgalactosidase μ staining

Sections from nestin-CreER^{T2} × lacZ lines were rinsed with TBS to remove residual antifreeze solution before being mounted onto slides and air-dried overnight. The next day, the sections were rehydrated in running tap water for 5 min, followed by incubation in PBS

containing 2 mM $MgCl_2$ for 15 min at room temperature. Slides were then transferred to pre-warmed 0.1 M phosphate buffer containing 2 mM $MgCl_2$, 0.2% Nonidet P-40, and 0.1% sodium deoxycholate for 10 min at 37° C. Slides were next incubated in X-gal staining solution overnight at 37° C in the dark [0.1 M $NaPO_4$, 5 mM K4Fe(CN)$_6$ (Sigma P3289), 5 mM $K_3Fe(CN)_6$ (Sigma 455946), 2 mM $MgCl_2$, 0.2% Nonidet P-40, 0.1% sodium deoxycholate, and 1.5 mM 5-bromo-4-chloro-3-indolyl-β-D-galactopyranoside (X-gal, 5 Prime, 2500040)]. The reaction was terminated by rinsing the slides 3 times at room temperature with 1× HEPES-buffered saline containing 0.1% Triton X-100 and 1 mM EDTA. The sections were post-fixed in 4% PFA for ≥ 1 hour at 4° C, rinsed with PBS to remove excess PFA, dehydrated through xylene, then rehydrated for counterstaining with a dilute solution of Nuclear Fast Red (0.03% Nuclear fast red kernechtrot (Fluka # 60700) and 1.67% $Al_2(SO_4)_3$ (Mallinckrodt # 3208)). Sections were again dehydrated into xylene and mounted with Permount (Fisher).

Microscopy

Bright field images were collected using a Zeiss AxioImager.Z1 microscope and AxioCam HRc digital camera. Fluorescence images were collected using the same microscope with a AxioCam MRm digital camera. Tiled images covering the full area of the tissue were collected at 5× magnification. High magnification fluorescence images were taken at 10× or 40× magnification using a Zeiss Apotome optical sectioning device and are shown here as compressed Z-stacks. All images were captured using Zeiss AxioVision 4.7 software. Figures were compiled using Adobe Photoshop CS6 (Adobe Systems), including adjustment of input:output levels within individual panels to optimize the signal for illustration.

Quantitation of recombination efficiency in GluCl reporter lines

Three sections containing the dorsal hippocampus (corresponding to horizontal plate numbers 154, 155, and 157 of the 3rd edition Franklin and Paxinos mouse brain atlas (Franklin and Paxinos, 2008)) were collected from each animal and co-immunostained for YFP and nestin as described above (n=4-5 per genotype). Overlapping Z-stack images were collected along the entire dentate gyrus of each section at 20× magnification. Nestin-positive cells were identified by the presence of immunolabeling that could be traced to a single DAPI-labeled nucleus within the SGZ and inner third of the GCL; YFP labeling in the green channel was then examined with nestin staining in the red to ascertain co-expression. Cells were manually counted within each field across both hemispheres and the total population of nestin-positive and the fraction of YFP-co-labeled cells for each animal reported here. Statistical comparison of recombination efficiency between lines was done by one-way ANOVA followed by Tukey post hoc analysis using Prism 6.0 software (GraphPad Software).

Results

Currently, nine different nestin-CreER^{T2} lines have been published, of which most are capable of driving expression in the SVZ (reviewed in (Imayoshi et al., 2011), see also (Dranovsky et al., 2011)). Here we focus on a subset of these lines shown to also drive expression in the SGZ: line K (Lagace et al., 2007), line H (named “H” after the donating

investigator solely as means of distinguishing this line for discussion) (Dranovsky et al., 2011), and line 4 (Imayoshi et al., 2006). We examined the specificity and efficiency of tamoxifen-induced recombination in each of these lines using three distinct Cre reporter strains: Ai3^{YFP} (Madisen et al., 2010), GluCl^{YFP} (described herein) and R26R^{LacZ} (Soriano, 1999). These reporters have all been targeted to the *ROSA26* locus, and while all use the endogenous promoter for transgene expression, Ai3 and GluCl additionally carry the strong artificial CAG promoter (Table 2). The reporters also differ in the length of the 'stop cassette' that must be removed to initiate reporter expression, with R26R and GluCl sharing a 2.7 kb sequence and Ai3 a shorter 0.9 kb stop. These features strongly influence the apparent CreER^{T2} expression indicated by each reporter and collectively offer a broad view of the expression patterns possible with each driver line. All animals used in the study were handled similarly: at 8 weeks of age, each mouse was injected with either vehicle or tamoxifen (180 mg/kg) once per day for five days; brains were harvested one week after the final injection. The resulting expression patterns are thus normalized for the animals' age, the age of the progenitor cells, and the total amount of tamoxifen delivered, yet the inherent differences far outweigh their superficial similarities.

Reporter expression in line K nestin-CreER^{T2} mice is highly specific but has limited efficiency

Line K generated by Lagace et al. was one of the first nestin-CreER^{T2} lines to permit recombination within neural progenitor cells of the SGZ (Lagace et al., 2007). As a result, this line has been widely used to manipulate the expression of proteins involved in hippocampal neurogenesis (Ables et al., 2010; Gao et al., 2009; Guo et al., 2011; Lagace et al., 2008; Teixeira et al., 2012). We confirmed that this line evoked Cre-mediated recombination that was largely restricted to the SGZ and SVZ of reporter lines Ai3 and R26R (Figure 1). Sparse YFP-positive cells with the morphology of astrocytes or mature neurons were occasionally found outside of these areas in tamoxifen-treated mice, however, they were only observed in the highly sensitive Ai3 reporter and comprised only a minor population of the labeled cells in this line. Consistent with this qualitative observation, semi-quantitative counts of ectopic labeling in selected regions of the hippocampus and cortex detected YFP expression in less than 0.5% of the total cell population (Table 3). Labeling was strictly limited to the SGZ (Figure 2) and SVZ/OB (Figure 3) in K × R26R animals, but was far less efficient with fewer positive cells showing evidence of CreER^{T2} activation than in the Ai3 reporter. In the absence of tamoxifen only K × Ai3 showed any evidence of recombination, where it was limited to the ventricular lining and appeared to label stationary ependymal cells rather than migratory progenitors.

The drop in recombination efficiency between Ai3 and R26R reporters suggested that line K became less effective as the distance between loxP sites increased from 0.9 to 2.7 kb (Table 2). We did not, however, anticipate the near total absence of recombination observed in the GluCl animals. This line was created primarily to express a modified form of the glutamate-gated chloride channel from *C. elegans* (GluCl) but was followed by a YFP cassette to label cells in which the channel was expressed. The construct shares features of both Ai3 and R26R reporters, using the same CAG promoter as Ai3 and the same loxP-flanked stop cassette as R26R. Its YFP cassette allowed us to use the GluCl line as an additional reporter

here that shared the stringent recombination of R26R, but which lacked the enzymatic amplification provided by the lacZ reaction. Under these more restrictive conditions, we observed no recombination in either SGZ (Figure 2) or SVZ (Figure 3). This reporter line thus serves as a counterpoint to Ai3 in framing the expected rates of recombination under high- and low-sensitivity conditions.

Line H produces strong expression in neurogenic regions and elsewhere

The nestin-CreER^{T2} created by Dranovsky and colleagues is a more recent addition to the growing collection of driver lines capable of inducing recombination within hippocampal neural progenitors (Dranovsky et al., 2011; Sahay et al., 2011a). Line H displayed strong recombination within both major neurogenic areas when crossed with either of the two traditional Cre reporters, Ai3 and R26R (Figures 1-3). Abundant YFP- or lacZ-positive cells were found in the SVZ and olfactory bulb (Figure 3). Labeling was most prominent at the termination of the rostral migratory stream, with positive cells filling the medial zone of the olfactory granule cell layer and scattered throughout the glomeruli. Intense labeling was also seen throughout the hippocampal SGZ, particularly in the Ai3 reporter, where labeled cells blanketed the inner third of the granule cell layer (Figure 2).

The most striking feature of reporter expression in line H expression was the degree of ectopic labeling observed in the Ai3 and R26R lines following tamoxifen treatment (Figures 1 and 2). Reporter expression was present throughout the deep layers of neocortex and pyramidal layers of hippocampus, with particularly strong expression in CA1 (Figure 1). Ectopic labeling reached as high as 50% of CA1, and nearly a quarter of all cells in temporal cortex L5 (Table 3). In both regions, labeling appeared primarily in neurons, which in many cases could be identified by location or morphology as pyramidal cells. Sparse labeling was also noted in striatum and thalamus, where a subset of the labeled cells had a distinctive snowflake-like shape suggestive of astroglia. Supporting a glial identity, cells of similar morphology expressed S100B in Line 4 × Ai3. Of note, these cells were also present in H × Ai3 mice without tamoxifen, while reporter expression in cells of neuronal morphology was much more tightly dependent on drug activation.

The most unexpected and overt ectopic expression occurred in the cerebellum, where we observed nearly complete labeling of the granule cell layer in all three reporter lines (Figures 1 and 4). Even the generally low-expressing GluCl reporter showed strong and consistent labeling within the cerebellum, despite relatively weak expression in the SGZ (Figure 2) and SVZ (Figure 3) and no sign of ectopic expression anywhere in the forebrain (Figure 1). Occasional Purkinje neurons were also labeled in the stronger reporters Ai3 and R26R, along with sparse small cells in the molecular layer consistent with interneurons (Figure 4). Like other neurons labeled in line H, expression was strictly dependent on tamoxifen, suggesting that the cerebellar expression was the result of CreER^{T2} present in the mature neurons at the time of injection.

Reporter expression in nestin-CreER^{T2} line 4 shares the striking cerebellar expression of line H

Imayoshi et al. characterized three nestin-CreER^{T2} lines for genetic manipulation of neural progenitor cells. The three lines differed in their ability to induce recombination within the mature brain, and of the set, line 4 was found to offer the best efficiency within SGZ (Imayoshi et al., 2006; Imayoshi et al., 2008). Consistent with this description, line 4 was notable in being able to induce expression even in the stringent GluCl-YFP reporter, where YFP-positive cells were found in SGZ, SVZ, and olfactory bulb (Figures 2 and 3). We also observed strong expression within both SGZ and SVZ of Ai3 and R26R reporters (Figures 1-3). Expression was especially strong within the olfactory bulb, where YFP- and lacZ-positive cells were found throughout the granule cell layer and densely invading the glomeruli (Figure 3). In the Ai3 reporter, dense networks of neuronal processes could be seen extending from the newborn granule neurons into the external plexiform layer. The dense glomerular labeling in the 4 × Ai3 mice suggests that recombination in this line started shortly after exposure to tamoxifen. This is further supported by the presence of a substantial number of cells in the SGZ with early dendritic processes extending into the molecular layer (Figure 2), consistent with the morphology of immature neurons 10 and 14 days after labeling (Zhao et al., 2006).

Similar to line H, line 4 also displayed a substantial degree of labeling outside the main neurogenic regions following tamoxifen treatment of 4 × Ai3 and 4 × R26R animals. Labeled cells were present in every brain region examined, including cortex, hippocampus (CA1-CA3), striatum, and thalamus (Figure 1). The most surprising cells to display YFP expression in Ai3 following tamoxifen treatment expression had the appearance of vascular endothelial cells or pericytes. These cells provided a fluorescent outline of the capillary bed throughout the forebrain, including cortex, hippocampus, and striatum. Immunostaining for collagen IV placed these cells within the basal lamina, but was not able to discern whether the YFP-positive cells were pericytes or endothelial cells (Figure 5). Consistent with this finding, semi-quantitative counts of labeled cells in temporal cortex and hippocampus showed that approximately 10% of the cell population expressed YFP in these areas, and most of those cells were non-neuronal (Table 3). Vascular labeling was not observed in the R26R reporter, and with the exception of the cerebellum, ectopic expression was much less extensive in this line. Like line H, line 4 induced extensive recombination with cerebellar granule neurons of all three reporter lines (Figure 4). Line 4 also induced expression within a significant fraction of Purkinje neurons of the Ai3 and R26R reporters (Figure 4).

Of the three nestin-CreER^{T2} lines tested, line 4 was associated with the highest degree of tamoxifen-independent reporter expression (Figure 1). This leak was most apparent in the highly sensitive Ai3 reporter, but could also be seen in many brain regions with R26R although to a much lesser degree. Vehicle-treated 4 × Ai3 animals also harbored many YFP-positive Purkinje neurons, likely contributing to the labeling of these cells in tamoxifen-treated animals (Figure 4). Tamoxifen-independent YFP expression was also observed in scattered pyramidal neurons throughout the cortex and hippocampus (CA1-CA3), mature granule neurons in the dentate gyrus, and interneurons of the cerebellar molecular layer. Additional YFP-positive cells with the ramified morphology of astrocytes were found in

every brain region examined. Immunostaining with S100B offered additional evidence for their identification as astrocytes (Figure 5). Compared to the Ai3 reporter, tamoxifen-independent expression was much less pronounced in R26R, and completely absent in GluCl. Expression in vehicle-treated R26R mice was most concentrated in the thalamus, however scattered positive cells could be found throughout the brain, resembling a subset of the pattern observed in Ai3.

Quantitative comparison of recombination efficiency confirms that line 4 labels the highest percentage of SGZ progenitors

In order to directly compare how much of the progenitor pool was labeled by each nestin-CreER^{T2} line following tamoxifen treatment, we manually counted the number of nestin-positive cells in the SGZ and determined how many were also co-labeled for YFP (Figure 2). We chose to study the GluCl reporter because it showed the greatest difference in labeling between the three lines and thus provided the widest range for comparison. Our analysis focused on sections from dorsal hippocampus as this region has a higher density of nestin-positive cells than ventral (Jinno, 2011). We found that all three lines showed equal numbers of nestin-positive cells (total nestin-positive cells counted: line 4: 774±54, line H: 743±95, line K: 737±145; ANOVA $p = 0.97$). While the target population was similar across lines, the percentage of progenitors labeled in each line was not. Line 4 showed the greatest efficiency, labeling 33 ± 0.6% of the nestin-positive cells in SGZ. Line K showed the lowest percentage of co-labeled cells, at 2.1 ± 0.9%. Line H was intermediate to the other two, with 18.9 ± 6.4% recombination efficiency (ANOVA for genotype: $p = 0.003$, Tukey post-hoc: 4 vs. K, $p = 0.002$; H vs. K, $p = 0.05$; 4 vs. H, $p = 0.11$). Of the three, line H was the only one in which we noted the suggestion of gender bias. The two female H × GluCl-YFP animals carried substantially more co-labeled cells than the three males we tested, however, the difference was not statistically significant due to the small sample size (Student's t-test, $p=0.098$). The percentages we report for the GluCl line are lower than would be observed in more sensitive strains such as Ai3 or R26R, but provide an accurate reflection of relative efficiency between the lines: 4 > H > K.

Discussion

Our study revealed a significant variation in the pattern of reporter expression induced by different nestin-CreER^{T2} transgenic lines. We found that each line produced recombination within known neurogenic regions of the adult brain, although they differed substantially in their efficacy. However, it was the specificity with which they labeled adult-born neurons rather than their efficiency that most distinguished the lines. Of the three we tested, line K was the only one that effectively limited expression to adult-born neurons, while lines H and 4 displayed a surprising degree of ectopic expression that had not been previously appreciated.

Both the efficiency and specificity of these nestin-CreER^{T2} lines may influence their experimental use. On one hand, cell lineage studies may be more forgiving of ectopic expression, provided there is some way to distinguish between the progeny of neural progenitors and other cells that were erroneously labeled. For example, studies of cell fate in

the SGZ would be unaffected by ectopic labeling in mature neurons of the cerebellum (Dranovsky et al., 2011; Imayoshi et al., 2008). Cell lineage studies would also be tolerant of lines in which recombination labeled only a partial subset of the neural progenitors, provided that all cells in the population were equipotent (Lagace et al., 2007). On the other hand, specificity and efficiency are considerably more important for behavioral studies, where expression outside of the intended population, or conversely, non-recombined cells within the population, may influence the results. In these cases, ectopic expression could be overcome by adding a second layer of spatial specificity, such as stereotaxic injection of genes under control of flip-excision switch (FLEX) elements to limit transgene expression within the radius of viral spread (Atasoy et al., 2008). Alternatively, optogenetic systems also incorporate secondary spatial control via light activation, which is limited by the position of the fiber optic and the point spread of its output. This approach was used by Kheirbek et al. to distinguish the function of dorsal from ventral hippocampus in animals that expressed optogenetic transgenes throughout the dentate gyrus, and by Gu et al. to silence adult-born neurons at critical stages in their maturation (Gu et al., 2012; Kheirbek et al., 2013). Without some means of imposing additional specificity, behavioral experiments using nestin-CreER^{T2} drivers with the potential for ectopic expression should be interpreted with caution.

Another factor that may determine which of the nestin-CreER^{T2} lines is most appropriate for a particular experimental situation is the precise developmental stage at which the transgene becomes active. Endogenous nestin protein is expressed by both type I radial glial cells and by the type IIa and IIb neural precursor cells to which they give rise (Encinas et al., 2011; Kronenberg et al., 2003). Radial glial cells are the slowly dividing putative stem cell of the niche and can be distinguished by their expression of GFAP and brain lipid-binding protein (BLBP), while type II precursors are a more rapidly dividing, but ultimately exhaustible derivative identified by T-box brain gene 2 (Encinas et al., 2011; Hodge et al., 2008). This distinction can dramatically impact the size and composition of the cellular population that ultimately carries the desired genetic recombination in the weeks and months following tamoxifen induction. Although our study was not designed to identify which stage was labeled by each of the nestin-CreER^{T2} lines, past work by the Eisch group has demonstrated that line K labels both type I and type II cells in the SGZ (Decarolis et al., 2013; Lagace et al., 2007). The number and type of labeled cells changed over time, however, with an initial surge in cells expressing the reporter during the first month after tamoxifen injection due to the proliferation of type II cells, followed by the emergence of a smaller, but more stable cohort of labeled radial glial cells and mature neurons in months 2-6 (Decarolis et al., 2013). In contrast, line H was shown to drive recombination primarily in type I GFAP+/BLBP+ radial glial cells when examined 48 hours after tamoxifen administration (Dranovsky et al., 2011). Over the following 6 months, the number of reporter-labeled cells derived from this progenitor pool grew severalfold, primarily through an increased number of mature neurons which persisted at 1 year. In a similar manner, the number of reporter-expressing mature neurons in line 4 mice increased dramatically during the first 6 months after tamoxifen treatment and remained stable thereafter (Imayoshi et al., 2008). Labeled cells arose primarily from recombination within GFAP+ radial glial cells, with additional, albeit less prominent expression in type IIb or type III doublecortin-positive progenitors. Overall, these

studies suggest that lines H and 4 may be most effective in type I cells, while line K the best choice for studies of type II progenitors. All three lines ultimately produced a stable population of genetically modified mature neurons, although how quickly they reach this steady-state and what fraction of adult-born neurons carry the rearrangement may depend on which progenitors are most efficiently targeted.

Each of the nestin-CreER^{T2} lines we studied has been used in past work to estimate the fraction of mature granule cells generated by adult neurogenesis (Decarolis et al., 2013; Dranovsky et al., 2011; Imayoshi et al., 2008; Lagace et al., 2007). Similar measures have also been done using GLAST-CreER^{T2} to label dividing progenitors (Decarolis et al., 2013; Ninkovic et al., 2007). These studies varied widely in their estimates, from as little as 1% of the total DGC population to as much as 14%. The differences likely arise from several factors including the exact progenitor stage at which CreER^{T2} is active and the efficiency with which it then induces reporter expression. The highest estimates would be expected from CreER^{T2} lines that are active in the earliest type I progenitors. Consistent with this, Imayoshi et al. reported that adult neurogenesis contributed 10% of the mature GCL in adult mice from line 4 (Imayoshi et al., 2008). Conversely, line K which appears to be more active in type II progenitors yielded a considerably lower estimate of this population (Lagace et al., 2007). Our findings generally align with these outcomes, but with only one week between the final tamoxifen injection and harvest, we can provide little insight into which estimate best reflects the life-long accrual of adult-born neurons. The varying estimates obtained by additive labeling of progenitors and progeny indicate that their contribution might be more accurate to measure subtractively. Rather than using a line in which CreER^{T2} is expressed in progenitors, a subtractive approach would use a line such as CaMKIIα-CreER^{T2} in which CreER^{T2} is active in mature neurons to completely label embryonic-born neurons in juvenile mice. The contribution of adult neurogenesis to the GCL at later ages could then be estimated by dividing the number of unlabeled mature neurons born (NeuN+/reporter-) by the total number of NeuN+ cells. While this subtractive approach may have technical pitfalls of its own, it avoids the major issues that have confounded estimates of additive labeling with nestin-CreER^{T2} lines.

The differences in specificity and efficiency between these three nestin-CreER^{T2} lines arose through a combination of design and chance. All three lines trace their CreER^{T2} sequence to the same study by Chambon and colleagues (Feil et al., 1997). In contrast, the lines differ significantly in the design of their *nestin* promoters (Table 4). The widest expressing line, line H, was constructed using a 5.4 kb rat genomic fragment containing the basal *nestin* promoter placed upstream of CreER^{T2}, and a 0.65 kb region of the *nestin* second intron placed in reverse orientation downstream of the poly-adenylation sequence (based on the pNERV vector, (Panchision et al., 2001); A. Dranovsky, personal communication). Our current findings suggest that these fragments of the endogenous sequence may convey the neural specificity, but not the temporal specificity, of the innate nestin gene.

Consistent with the slightly more restricted expression of line 4, Imayoshi et al. used a construct generated by Enikolapov and colleagues which contained 5.8 kb of the rat *nestin* promoter plus a 1.8 kb fragment spanning the entire second intron, both cloned in their original orientation (Mignone et al., 2004). In our hands, this line showed substantial

expression within granule neurons and Purkinje cells of the cerebellum in addition to cells of glial morphology throughout the brain. In contrast, when the same construct was used to directly control a GFP reporter, expression was limited to the SGZ, SVZ, rostral migratory stream, and olfactory bulb. No ectopic expression was observed in either neurons or glia (Mignone et al., 2004). At least two factors may contribute to the appearance of ectopic expression in the nestin-CreER^{T2} mice made from the Enikolapov construct. First, *nestin* is a fairly weak promoter. When used to directly control reporter protein, only the most highly expressing cells will produce enough GFP to appear labeled. In contrast, visualizing transgene expression in the CreER^{T2} line requires an intermediate reporter such as R26R or Ai3. Once the stop cassette is excised, these reporters depend on their own much stronger promoters, ROSA26 and CAG, respectively, to drive expression of the detected protein. We may simply get a more sensitive view of *nestin* expression using an amplifying reporter than we do with direct GFP expression. The second possibility is that the integration site of the transgene influences its specificity. This conclusion is supported by the variation in CreER^{T2} expression observed in other nestin-CreER^{T2} lines generated using the same construct alongside line 4. Of seven founders produced, the highest expressing line drove lacZ reporter expression throughout the CNS even in the absence of tamoxifen (Imayoshi et al., 2006). Line 4, expressing an intermediate level of CreER^{T2} mRNA, displayed considerably less tamoxifen-independent lacZ expression that was limited to the ventricular zone of the developing CNS. The line with lowest CreER^{T2} expression, line 5-1, provided the greatest specificity, but conversely, was later shown to have low recombination efficiency in the adult SGZ (Imayoshi et al., 2008). These expression differences suggest that in addition to the nestin elements used for patterning, the genomic environment in which each transgene lands can profoundly influence its expression.

In contrast to the strong but widespread expression noted in Lines H and 4, reporter expression in line K was strictly limited to progenitor cells in the SGZ and SVZ. Compared to the other lines, Eisch and colleagues incorporated considerably more of the rat *nestin* gene into their transgene construct. The Xh5 vector they used, created by Piccioto and colleagues, contains the 5.8 kb *nestin* promoter, along with 5.4 kb of downstream sequence including part of exons 1 and 4, all of exons 2 and 3, and the complete sequence of the three intervening introns ((Beech et al., 2004) with reference to (Lendahl et al., 1990; Zimmerman et al., 1994)). Thus, line K shared the same promoter sequence as line 4 and the same second intron, but also carried the remaining two introns plus at least partial sequence from all 4 exons. This suggests that elements outside of the second intron may be critical for temporal restriction. Resolving the endogenous expression pattern in the adult brain will await the creation of a knock-in line expressing CreER^{T2}, ideally alongside a fluorescent reporter. Line K was the only line we tested that did not display prominent expression in the cerebellum, a trait that lines H and 4 share with other nestin-CreER^{T2} lines described in the literature (Alcantara Llaguno et al., 2009; Chen et al., 2009). However, the relatively weak recombination efficiency of line K within the SVZ and SGZ compared with lines 4 and H also suggest that the larger transgene of line K may have incorporated with fewer copies, making it less effective at excising DNA between loxP sites spaced more than 1 kb apart (see discussion below).

Our study further demonstrates that the sensitivity of the reporter line also affects the apparent expression pattern observed for each Cre driver. The three reporter lines we tested were all targeted to the *ROSA26* genomic locus which is widely used for its near-ubiquitous expression capability and normal phenotype when inactivated (Soriano, 1999). However, only one of our three reporter strains relied on the endogenous *ROSA26* promoter for expression. Both the Ai3 and GluCl reporters included the strong CAG hybrid promoter in the targeting construct to enhance mRNA expression following recombination. While the boost provided by the added CAG promoter was sufficient to allow visualization of the native transgene in the Ai3 offspring, it appears that translation of the multi-cistronic mRNA (3.5 kb) may have limited YFP levels in the GluCl line and thereby dampened its fluorescence. The other major factor governing the sensitivity of the reporters we tested is the length of intervening sequence between loxP sites (Morozov, 2008). The most sensitive of the reporters, Ai3, was also the one with the shortest stop cassette (900 bp; Hongkui Zeng, personal communication). In contrast, our GluCl line used a much larger stop cassette of 2.7 kb derived from the same constructs used to make the R26R line (Soriano, 1999; Srinivas et al., 2001). The longer stop cassette likely contributed to the limited recombination observed in our GluCl line compared to Ai3. However, the size of the stop cassette does not explain the lower sensitivity of GluCl compared to R26R. Instead, the enzymatic detection used for the lacZ reporter may have increased our ability to see recombination in R26R that was below the threshold of detection by YFP immunofluorescence in GluCl.

Our findings suggest that each CreER^{T2} and loxP-flanked target should be assessed independently to fully understand whether the expression pattern attained is appropriate for the experiments planned. While in many cases there may be limited options available for the target allele, there are a growing number of inducible CreER^{T2} lines that may be useful in cases where nestin-CreER^{T2} is not. The temporally-specific patterns of proteins such as Sox2 (Favaro et al., 2009; Kang and Hebert, 2012), Doublecortin (Cheng et al., 2011; Zhang et al., 2010b), Ascl1 (Battiste et al., 2007), TLX (Liu et al., 2008), and Gli1 (Ahn and Joyner, 2004) have been used to create CreER^{T2} lines capable of directing recombination in either embryonic or adult-born neurons. Genetic intersectional strategies combining CreER^{T2} with flippase/frt (Dymecki et al., 2010), or physical strategies combining Cre or CreER^{T2} with stereotaxically-injected viral elements (Zhang et al., 2010a), may allow further selectivity where needed. Given the remarkable proliferation of genetic strategies for manipulating protein expression within adult-born neurons that have been published within just the last 5 to 10 years, we already have the tools in hand to overcome many experimental obstacles provided we are careful enough to recognize them in the first place.

Acknowledgments

We thank Bryan Song and Anna Kuperman for animal care, Andy Groves and Stacy Grunke for comments on the manuscript, Roy Sillitoe for advice and reagents to identify cerebellar interneurons, Brendan Lee for helping us to establish the B6 GluCl-YFP line, Amelia Eisch for sharing nestin-CreER^{T2} line K, Rene Hen for sharing nestin-CreER^{T2} line “H”, Ryochiro Kageyama for allowing use of nestin-CreER^{T2} line 4, and Michael Drew for sharing embryos from line 4.

Grant sponsor: National Institutes of Health (NIH) Office of the Director, Grant number: DP2 OD001734 (to JLJ); Grant sponsor: National Institute of Mental Health (NIMH), Grant number R21MH101583 (to JLJ); Grant sponsor:

National Institute of Aging, Grant number: T32 AG000183 (support for MJY). Grant sponsor: Robert and Renee Belfer Family Foundation, Grant number: Neurodegeneration Consortium (NDC). Grant sponsor: *Eunice Kennedy Shriver* National Institute of Child Health and Human Development (NICHD), Grant number: 5P30HD024064-25 (to Dr. Huda Zoghbi, support for BCM ES cell core).

Role of Authors

MYS generated the mice for analysis and conducted all tamoxifen experiments, MJY assisted with colony maintenance and data interpretation, TCL made the GluCl-YFP targeting construct and screened ES clones, YL performed blastocyst injections and embryo transfer, and JLJ designed the study and wrote the manuscript.

Abbreviations

DGC	dentate granule cell
GluCl	glutamate-gated chloride channel
NPC	neural progenitor cell
OB	olfactory bulb
SGZ	subgranular zone
SVZ	subventricular zone
WPRE	woodchuck hepatitis virus posttranscriptional regulatory element
YFP	yellow fluorescent protein

References

Ables JL, Decarolis NA, Johnson MA, Rivera PD, Gao Z, Cooper DC, Radtke F, Hsieh J, Eisch AJ. Notch1 is required for maintenance of the reservoir of adult hippocampal stem cells. J Neurosci. 2010; 30(31):10484–10492. [PubMed: 20685991]

Ahn S, Joyner AL. Dynamic changes in the response of cells to positive hedgehog signaling during mouse limb patterning. Cell. 2004; 118(4):505–516. [PubMed: 15315762]

Aimone JB, Deng W, Gage FH. Resolving new memories: a critical look at the dentate gyrus, adult neurogenesis, and pattern separation. Neuron. 2011; 70(4):589–596. [PubMed: 21609818]

Aimone JB, Wiles J, Gage FH. Potential role for adult neurogenesis in the encoding of time in new memories. Nat Neurosci. 2006; 9(6):723–727. [PubMed: 16732202]

Alcantara Llaguno S, Chen J, Kwon CH, Jackson EL, Li Y, Burns DK, Alvarez-Buylla A, Parada LF. Malignant astrocytomas originate from neural stem/progenitor cells in a somatic tumor suppressor mouse model. Cancer cell. 2009; 15(1):45–56. [PubMed: 19111880]

Arruda-Carvalho M, Sakaguchi M, Akers KG, Josselyn SA, Frankland PW. Posttraining ablation of adult-generated neurons degrades previously acquired memories. J Neurosci. 2011; 31(42):15113–15127. [PubMed: 22016545]

Atasoy D, Aponte Y, Su HH, Sternson SM. A FLEX switch targets Channelrhodopsin-2 to multiple cell types for imaging and long-range circuit mapping. J Neurosci. 2008; 28(28):7025–7030. [PubMed: 18614669]

Battiste J, Helms AW, Kim EJ, Savage TK, Lagace DC, Mandyam CD, Eisch AJ, Miyoshi G, Johnson JE. Ascl1 defines sequentially generated lineage-restricted neuronal and oligodendrocyte precursor cells in the spinal cord. Development. 2007; 134(2):285–293. [PubMed: 17166924]

Beech RD, Cleary MA, Treloar HB, Eisch AJ, Harrist AV, Zhong W, Greer CA, Duman RS, Picciotto MR. Nestin promoter/enhancer directs transgene expression to precursors of adult generated periglomerular neurons. J Comp Neurol. 2004; 475(1):128–141. [PubMed: 15176089]

Chen J, Kwon CH, Lin L, Li Y, Parada LF. Inducible site-specific recombination in neural stem/progenitor cells. Genesis. 2009; 47(2):122–131. [PubMed: 19117051]

Cheng X, Li Y, Huang Y, Feng X, Feng G, Xiong ZQ. Pulse labeling and long-term tracing of newborn neurons in the adult subgranular zone. Cell research. 2011; 21(2):338–349. [PubMed: 20938464]

Decarolis NA, Mechanic M, Petrik D, Carlton A, Ables JL, Malhotra S, Bachoo R, Gotz M, Lagace DC, Eisch AJ. In vivo contribution of nestin- and GLAST-lineage cells to adult hippocampal neurogenesis. Hippocampus. 2013; 23(8):708–719. [PubMed: 23554226]

Deng W, Aimone JB, Gage FH. New neurons and new memories: how does adult hippocampal neurogenesis affect learning and memory? Nat Rev Neurosci. 2010; 11(5):339–350. [PubMed: 20354534]

Dranovsky A, Picchini AM, Moadel T, Sisti AC, Yamada A, Kimura S, Leonardo ED, Hen R. Experience dictates stem cell fate in the adult hippocampus. Neuron. 2011; 70(5):908–923. [PubMed: 21658584]

Dymecki SM, Ray RS, Kim JC. Mapping cell fate and function using recombinase-based intersectional strategies. Methods Enzymol. 2010; 477:183–213. [PubMed: 20699143]

Eisch AJ, Petrik D. Depression and hippocampal neurogenesis: a road to remission? Science. 2012; 338(6103):72–75. [PubMed: 23042885]

Encinas JM, Michurina TV, Peunova N, Park JH, Tordo J, Peterson DA, Fishell G, Koulakov A, Enikolopov G. Division-coupled astrocytic differentiation and age-related depletion of neural stem cells in the adult hippocampus. Cell stem cell. 2011; 8(5):566–579. [PubMed: 21549330]

Favaro R, Valotta M, Ferri AL, Latorre E, Mariani J, Giachino C, Lancini C, Tosetti V, Ottolenghi S, Taylor V, Nicolis SK. Hippocampal development and neural stem cell maintenance require Sox2-dependent regulation of Shh. Nat Neurosci. 2009; 12(10):1248–1256. [PubMed: 19734891]

Feil R, Wagner J, Metzger D, Chambon P. Regulation of Cre recombinase activity by mutated estrogen receptor ligand-binding domains. Biochem Biophys Res Commun. 1997; 237(3):752–757. [PubMed: 9299439]

Franklin, KBJ.; Paxinos, G. The mouse brain in stereotaxic coordinates. Acadmic Press; San Diego, CA: 2008.

Gao Z, Ure K, Ables JL, Lagace DC, Nave KA, Goebbels S, Eisch AJ, Hsieh J. Neurod1 is essential for the survival and maturation of adult-born neurons. Nat Neurosci. 2009; 12(9):1090–1092. [PubMed: 19701197]

Gould E. How widespread is adult neurogenesis in mammals? Nat Rev Neurosci. 2007; 8(6):481–488. [PubMed: 17514200]

Gu Y, Arruda-Carvalho M, Wang J, Janoschka SR, Josselyn SA, Frankland PW, Ge S. Optical controlling reveals time-dependent roles for adult-born dentate granule cells. Nat Neurosci. 2012; 15(12):1700–1706. [PubMed: 23143513]

Guo W, Allan AM, Zong R, Zhang L, Johnson EB, Schaller EG, Murthy AC, Goggin SL, Eisch AJ, Oostra BA, Nelson DL, Jin P, Zhao X. Ablation of Fmrp in adult neural stem cells disrupts hippocampus-dependent learning. Nat Med. 2011; 17(5):559–565. [PubMed: 21516088]

Hockfield S, McKay RD. Identification of major cell classes in the developing mammalian nervous system. J Neurosci. 1985; 5(12):3310–3328. [PubMed: 4078630]

Hodge RD, Kowalczyk TD, Wolf SA, Encinas JM, Rippey C, Enikolopov G, Kempermann G, Hevner RF. Intermediate progenitors in adult hippocampal neurogenesis: Tbr2 expression and coordinate regulation of neuronal output. J Neurosci. 2008; 28(14):3707–3717. [PubMed: 18385329]

Huang Q, Zhou D, Sapp E, Aizawa H, Ge P, Bird ED, Vonsattel JP, DiFiglia M. Quinolinic acid-induced increases in calbindin D28k immunoreactivity in rat striatal neurons in vivo and in vitro mimic the pattern seen in Huntington's disease. Neuroscience. 1995; 65(2):397–407. [PubMed: 7777157]

Imayoshi I, Ohtsuka T, Metzger D, Chambon P, Kageyama R. Temporal regulation of Cre recombinase activity in neural stem cells. Genesis. 2006; 44(5):233–238. [PubMed: 16652364]

Imayoshi I, Sakamoto M, Kageyama R. Genetic methods to identify and manipulate newly born neurons in the adult brain. Frontiers in neuroscience. 2011; 5:64. [PubMed: 21562606]

Imayoshi I, Sakamoto M, Ohtsuka T, Takao K, Miyakawa T, Yamaguchi M, Mori K, Ikeda T, Itohara S, Kageyama R. Roles of continuous neurogenesis in the structural and functional integrity of the adult forebrain. Nat Neurosci. 2008; 11(10):1153–1161. [PubMed: 18758458]

Jinno S. Topographic differences in adult neurogenesis in the mouse hippocampus: a stereology-based study using endogenous markers. Hippocampus. 2011; 21(5):467–480. [PubMed: 20087889]

Kang W, Hebert JM. A Sox2 BAC transgenic approach for targeting adult neural stem cells. PloS one. 2012; 7(11):e49038. [PubMed: 23145058]

Kheirbek MA, Drew LJ, Burghardt NS, Costantini DO, Tannenholz L, Ahmari SE, Zeng H, Fenton AA, Hen R. Differential control of learning and anxiety along the dorsoventral axis of the dentate gyrus. Neuron. 2013; 77(5):955–968. [PubMed: 23473324]

Kronenberg G, Reuter K, Steiner B, Brandt MD, Jessberger S, Yamaguchi M, Kempermann G. Subpopulations of proliferating cells of the adult hippocampus respond differently to physiologic neurogenic stimuli. J Comp Neurol. 2003; 467(4):455–463. [PubMed: 14624480]

Lagace DC, Benavides DR, Kansy JW, Mapelli M, Greengard P, Bibb JA, Eisch AJ. Cdk5 is essential for adult hippocampal neurogenesis. Proc Natl Acad Sci U S A. 2008; 105(47):18567–18571. [PubMed: 19017796]

Lagace DC, Whitman MC, Noonan MA, Ables JL, DeCarolis NA, Arguello AA, Donovan MH, Fischer SJ, Farnbauch LA, Beech RD, DiLeone RJ, Greer CA, Mandyam CD, Eisch AJ. Dynamic contribution of nestin-expressing stem cells to adult neurogenesis. J Neurosci. 2007; 27(46): 12623–12629. [PubMed: 18003841]

Lendahl U, Zimmerman LB, McKay RD. CNS stem cells express a new class of intermediate filament protein. Cell. 1990; 60(4):585–595. [PubMed: 1689217]

Lerchner W, Xiao C, Nashmi R, Slimko EM, van Trigt L, Lester HA, Anderson DJ. Reversible silencing of neuronal excitability in behaving mice by a genetically targeted, ivermectin-gated Cl- channel. Neuron. 2007; 54(1):35–49. [PubMed: 17408576]

Liu HK, Belz T, Bock D, Takacs A, Wu H, Lichter P, Chai M, Schutz G. The nuclear receptor tailless is required for neurogenesis in the adult subventricular zone. Genes & development. 2008; 22(18): 2473–2478. [PubMed: 18794344]

Madisen L, Zwingman TA, Sunkin SM, Oh SW, Zariwala HA, Gu H, Ng LL, Palmiter RD, Hawrylycz MJ, Jones AR, Lein ES, Zeng H. A robust and high-throughput Cre reporting and characterization system for the whole mouse brain. Nat Neurosci. 2010; 13(1):133–140. [PubMed: 20023653]

Marin-Burgin A, Schinder AF. Requirement of adult-born neurons for hippocampus-dependent learning. Behav Brain Res. 2012; 227(2):391–399. [PubMed: 21763727]

Mignone JL, Kukekov V, Chiang AS, Steindler D, Enikolopov G. Neural stem and progenitor cells in nestin-GFP transgenic mice. J Comp Neurol. 2004; 469(3):311–324. [PubMed: 14730584]

Ming GL, Song H. Adult neurogenesis in the mammalian brain: significant answers and significant questions. Neuron. 2011; 70(4):687–702. [PubMed: 21609825]

Morozov A. Conditional gene expression and targeting in neuroscience research. Curr Protoc Neurosci. 2008 Chapter 4:Unit 4 31.

Niibori Y, Yu TS, Epp JR, Akers KG, Josselyn SA, Frankland PW. Suppression of adult neurogenesis impairs population coding of similar contexts in hippocampal CA3 region. Nature communications. 2012; 3:1253.

Ninkovic J, Mori T, Gotz M. Distinct modes of neuron addition in adult mouse neurogenesis. J Neurosci. 2007; 27(40):10906–10911. [PubMed: 17913924]

Panchision DM, Pickel JM, Studer L, Lee SH, Turner PA, Hazel TG, McKay RD. Sequential actions of BMP receptors control neural precursor cell production and fate. Genes & development. 2001; 15(16):2094–2110. [PubMed: 11511541]

Petrik D, Lagace DC, Eisch AJ. The neurogenesis hypothesis of affective and anxiety disorders: are we mistaking the scaffolding for the building? Neuropharmacology. 2012; 62(1):21–34. [PubMed: 21945290]

Pettitt SJ, Liang Q, Rairdan XY, Moran JL, Prosser HM, Beier DR, Lloyd KC, Bradley A, Skarnes WC. Agouti C57BL/6N embryonic stem cells for mouse genetic resources. Nat Methods. 2009; 6(7):493–495. [PubMed: 19525957]

Sahay A, Scobie KN, Hill AS, O'Carroll CM, Kheirbek MA, Burghardt NS, Fenton AA, Dranovsky A, Hen R. Increasing adult hippocampal neurogenesis is sufficient to improve pattern separation. Nature. 2011a; 472(7344):466–470. [PubMed: 21460835]

Sahay A, Wilson DA, Hen R. Pattern separation: a common function for new neurons in hippocampus and olfactory bulb. Neuron. 2011b; 70(4):582–588. [PubMed: 21609817]

Schwaller B, Meyer M, Schiffmann S. 'New' functions for 'old' proteins: the role of the calcium-binding proteins calbindin D-28k, calretinin and parvalbumin, in cerebellar physiology. Studies with knockout mice. Cerebellum. 2002; 1(4):241–258. [PubMed: 12879963]

Slimko EM, Lester HA. Codon optimization of Caenorhabditis elegans GluCl ion channel genes for mammalian cells dramatically improves expression levels. Journal of neuroscience methods. 2003; 124(1):75–81. [PubMed: 12648766]

Snyder JS, Cameron HA. Could adult hippocampal neurogenesis be relevant for human behavior? Behav Brain Res. 2012; 227(2):384–390. [PubMed: 21736900]

Soriano P. Generalized lacZ expression with the ROSA26 Cre reporter strain. Nat Genet. 1999; 21(1): 70–71. [PubMed: 9916792]

Srinivas S, Watanabe T, Lin CS, William CM, Tanabe Y, Jessell TM, Costantini F. Cre reporter strains produced by targeted insertion of EYFP and ECFP into the ROSA26 locus. BMC developmental biology. 2001; 1:4. [PubMed: 11299042]

Steiner J, Bernstein HG, Bielau H, Berndt A, Brisch R, Mawrin C, Keilhoff G, Bogerts B. Evidence for a wide extra-astrocytic distribution of S100B in human brain. BMC neuroscience. 2007; 8:2. [PubMed: 17199889]

Teixeira CM, Kron MM, Masachs N, Zhang H, Lagace DC, Martinez A, Reillo I, Duan X, Bosch C, Pujadas L, Brunso L, Song H, Eisch AJ, Borrell V, Howell BW, Parent JM, Soriano E. Cell-autonomous inactivation of the reelin pathway impairs adult neurogenesis in the hippocampus. J Neurosci. 2012; 32(35):12051–12065. [PubMed: 22933789]

Trichas G, Begbie J, Srinivas S. Use of the viral 2A peptide for bicistronic expression in transgenic mice. BMC Biol. 2008; 6:40. [PubMed: 18793381]

Urabe N, Naito I, Saito K, Yonezawa T, Sado Y, Yoshioka H, Kusachi S, Tsuji T, Ohtsuka A, Taguchi T, Murakami T, Ninomiya Y. Basement membrane type IV collagen molecules in the choroid plexus, pia mater and capillaries in the mouse brain. Archives of histology and cytology. 2002; 65(2):133–143. [PubMed: 12164337]

Yassa MA, Stark CE. Pattern separation in the hippocampus. Trends in neurosciences. 2011; 34(10): 515–525. [PubMed: 21788086]

Zhang F, Gradinaru V, Adamantidis AR, Durand R, Airan RD, de Lecea L, Deisseroth K. Optogenetic interrogation of neural circuits: technology for probing mammalian brain structures. Nat Protoc. 2010a; 5(3):439–456. [PubMed: 20203662]

Zhang J, Giesert F, Kloos K, Vogt Weisenhorn DM, Aigner L, Wurst W, Couillard-Despres S. A powerful transgenic tool for fate mapping and functional analysis of newly generated neurons. BMC neuroscience. 2010b; 11:158. [PubMed: 21194452]

Zhao C, Teng EM, Summers RG Jr. Ming GL, Gage FH. Distinct morphological stages of dentate granule neuron maturation in the adult mouse hippocampus. J Neurosci. 2006; 26(1):3–11. [PubMed: 16399667]

Zimmerman L, Parr B, Lendahl U, Cunningham M, McKay R, Gavin B, Mann J, Vassileva G, McMahon A. Independent regulatory elements in the nestin gene direct transgene expression to neural stem cells or muscle precursors. Neuron. 1994; 12(1):11–24. [PubMed: 8292356]

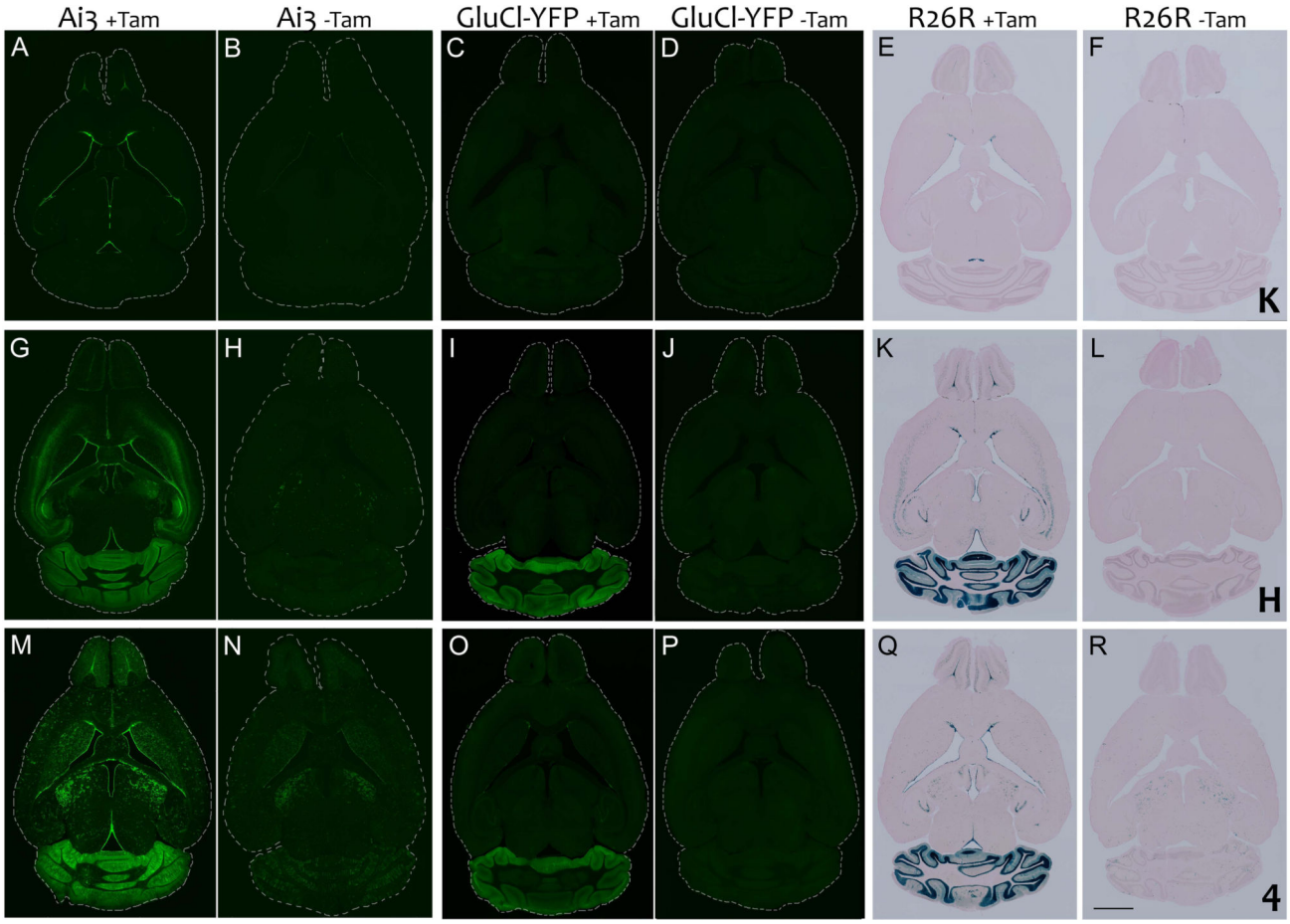

Figure 1. The efficiency and specificity of recombination vary substantially between three nestin-CreER^{T2} lines and also depend on the sensitivity of the reporter

Images show bigenic animals from nestin-CreER^{T2} lines K (panels A-F), H (panels G-L), and 4 (panels M-R) crossed with reporter lines Ai3, GluCl-YFP, and R26R. Animals were treated with tamoxifen (+ Tam; panels A, C, E, G, I, K, M, O, and Q)) or vehicle (−Tam; panels B, D, F, H, J, L, N, P, and R) for 5 days starting at 8 weeks of age, and harvested 7 days after the final injection. Expression in Ai3 animals is shown as native fluorescence (panels A, B, G, H, M, and N); YFP immunostaining for GluCl-YFP (panels C, D, I, J, O, and P) and β-galactosidase staining for R26R (panels E, F, K, L, Q, and R). In line K, reporter expression was almost entirely restricted to neurogenic areas: OB, SVZ and SGZ. In the absence of tamoxifen, the highly sensitive Ai3 reporter contained YFP+ cells at the ependymal lining of the lateral ventricle and very occasional YFP+ mature neurons in other brain areas, however no obvious reporter expression was detected in vehicle-treated R26R animals. Very little or no recombination was detected in the most stringent GluCl-YFP reporter with or without tamoxifen. In lines H and 4, strong reporter expression was detected in all major neurogenic areas following tamoxifen treatment. The most striking feature of these lines, however, was their strong cerebellar labeling which was seen in all three reporters. Ectopic expression was also observed in most other brain areas with the Ai3 reporter and to a lesser extent with R26R, notably in the cortex and hippocampus of line H and the thalamus and striatum of line K. In the absence of tamoxifen, both lines displayed

some leak that could be detected with Ai3 and to a lesser extent R26R. Tamoxifen-independent labeling was more prominent in line 4 than line H, and strongest in thalamus for both lines, with additional labeling of cerebellum and striatum in line 4. *Scale bar = 2 mm* A high resolution version of this figure can be found at wiley.biolucida.net.

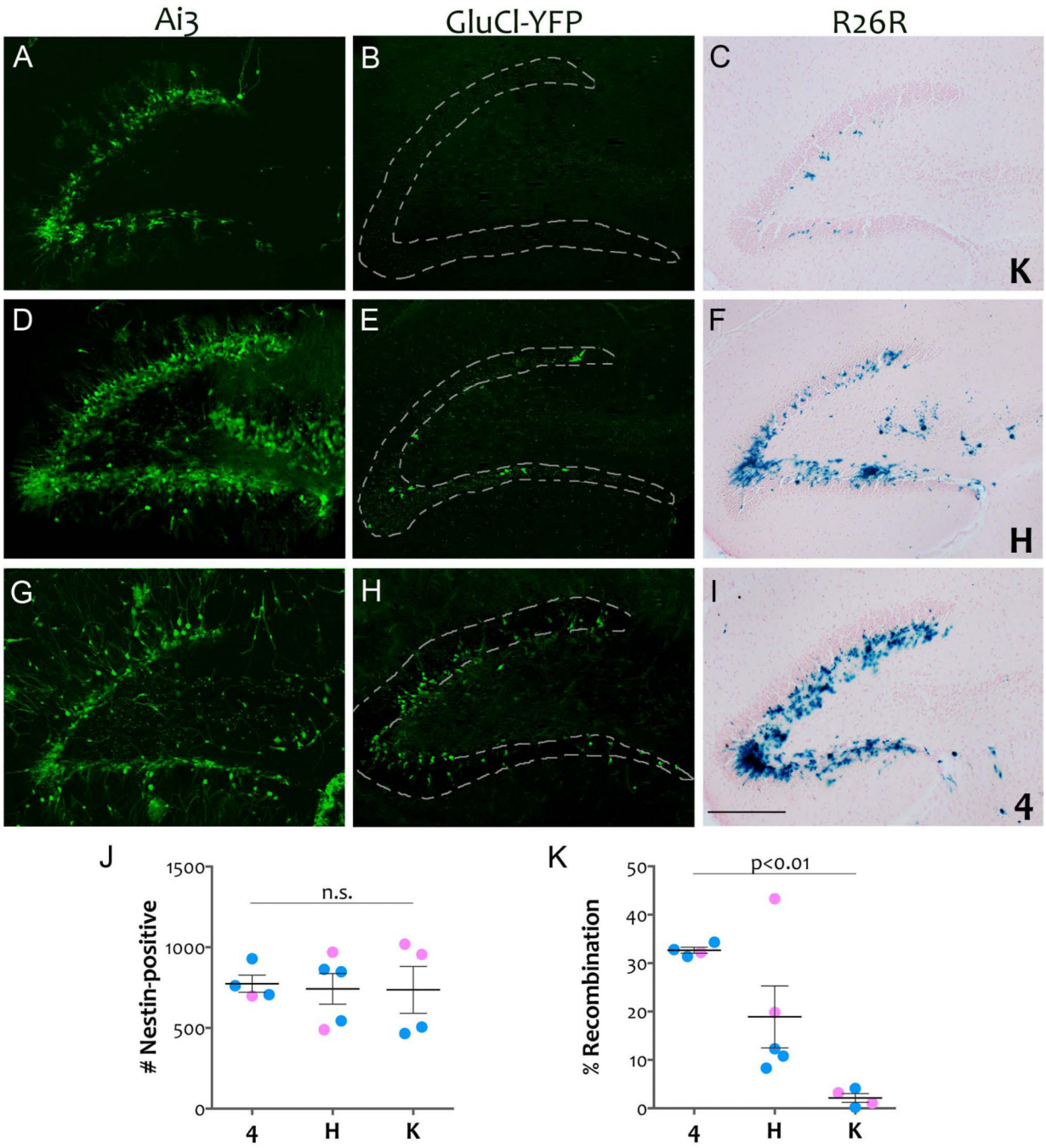

Figure 2. All three nestin-CreER^{T2} lines produce recombination within the SGZ

Tamoxifen-treated bigenic animals from each combination of driver lines K (panels A-C), H (panels D-F), and 4 (panels G-I) with responder lines Ai3, GluCl-YFP, and R26R were imaged for native YFP fluorescence (Ai3; panels A, D, and G) immunostained for YFP (GluCl-YFP; panels B, E, and H) or used for β-galactosidase detection (R26R; panels C, F, and I). The efficiency of recombination varied between the lines, however, all three were capable of inducing reporter expression within the SGZ. Reporter line Ai3 also reveals some ectopic expression within the hilus and CA3 of line H, while line 4 displayed some vascular

labeling and astrocytic labeling. Many of the labeled cells in 4 × Ai3 already have the morphology of immature neurons, suggesting that this driver becomes active soon after initial exposure to tamoxifen. *Scale bar = 200 μm*. The graphs show the total number of nestin-positive cells counted in the SGZ from 3 sections of dorsal hippocampus (panel J) and the percentage of nestin-positive cells that co-labeled for YFP in animals from the GluCl-YFP reporter crosses (panel K). While the nestin-positive population did not differ between the lines, the efficiency of recombination did, with line 4 showing the highest recombination in SGZ and line K the lowest. Pink = female, blue = male, lines reflect mean ± SEM.

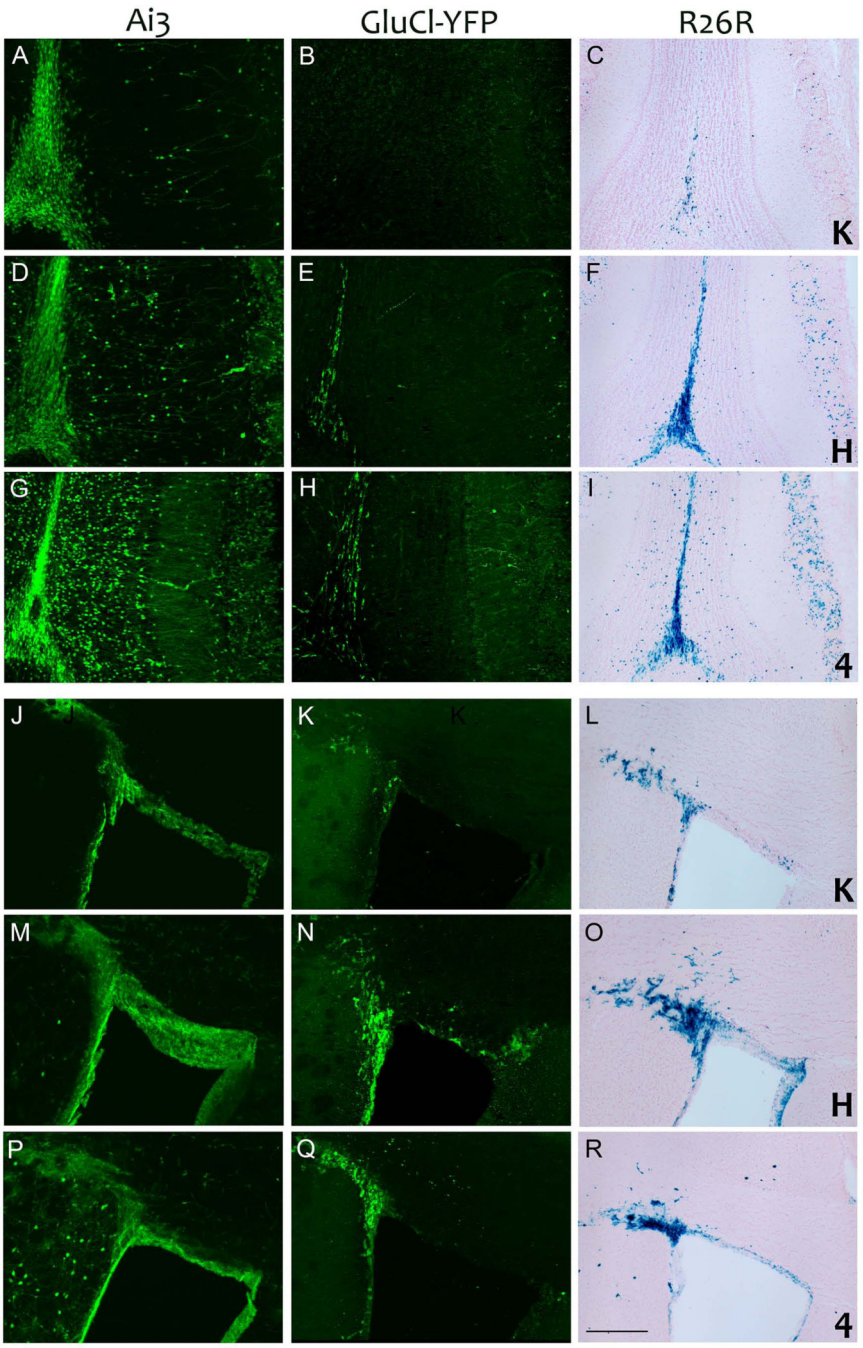

Figure 3. Nestin-CreER^{T2} line H drives SVZ progenitor cell recombination more strongly than lines 4 or K

Tamoxifen-treated bigenic animals from each combination of driver lines K (panels A-C and J-L), H (panels D-F and M-O), and 4 (panels G-I and P-R) with responder lines Ai3, GluCl-YFP, and R26R were imaged for native YFP fluorescence (Ai3; panels A, D, G, J, M and P) immunostained for YFP (GluCl-YFP; panels B, E, H, K, N, and Q) or used for β-galactosidase detection (R26R; panels C, F, I, L, O, and R). All three driver lines induced recombination in neural progenitor cells of the SVZ (panels J-R) leading to strong reporter expression in the rostral migratory stream and olfactory bulb (panels A-I). Line H was

somewhat more efficient in the SVZ than 4, although 4 likely became active earlier in the tamoxifen regimen as it displayed more labeled neurons in the terminal glomeruli than H. Both lines H and 4 yielded substantially stronger expression within the SVZ and rostral migratory stream than did line K. *Scale bar = 200 μm*

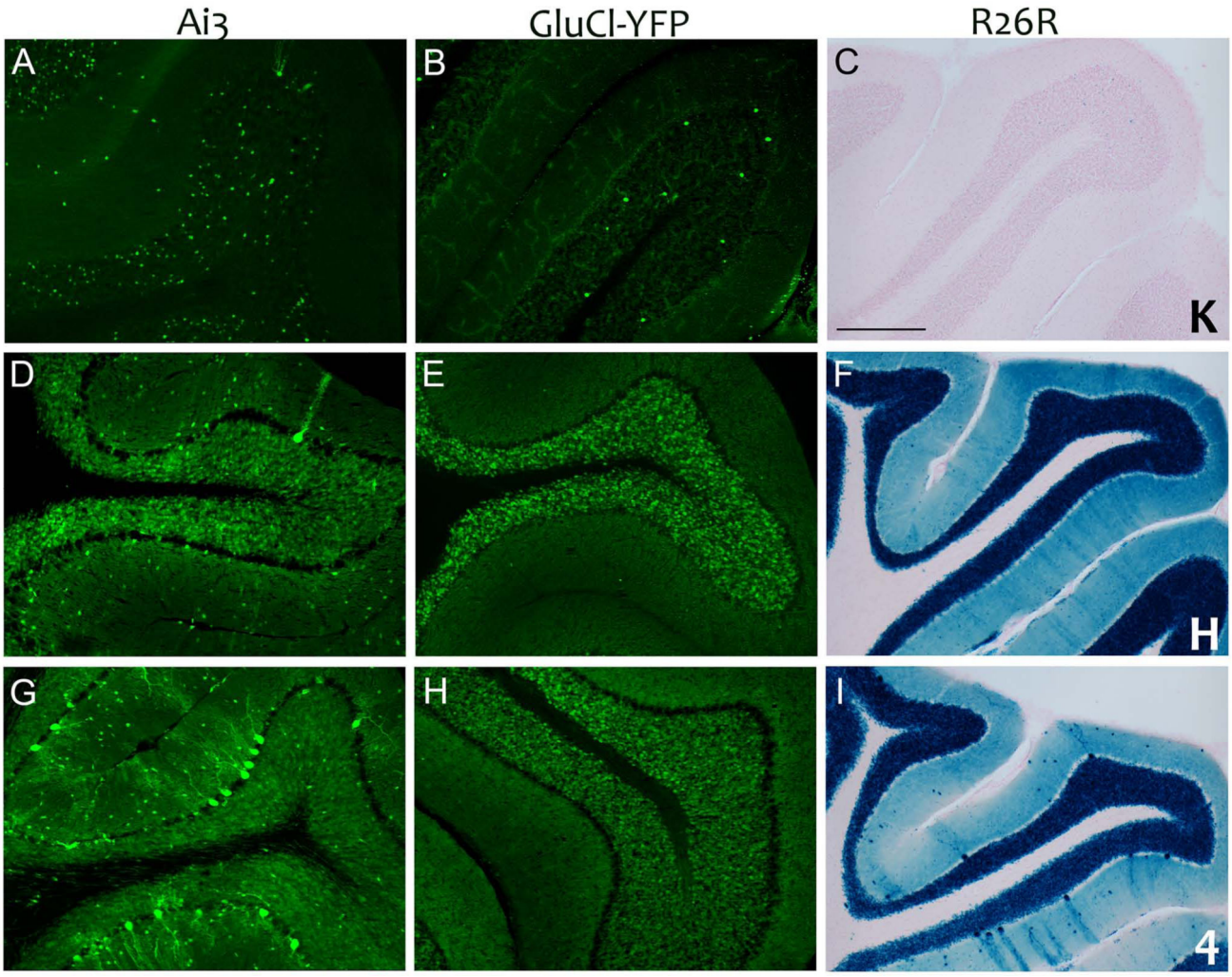

Figure 4. Nestin-CreER^{T2} lines 4 and H induce robust cerebellar recombination

High magnification images of cerebellar folia from tamoxifen-treated bigenic animals were imaged for native fluorescence (Ai3; panels A, D, and G), immunostained for YFP (GluCl-YFP; panels B, E, and H), or developed with X-gal (R26R; panels C, F, and I). While line K induced minimal recombination of granule cells in the cerebellum (panels A-C), strong granule cell labeling was noted in lines H (panels D-F) and 4 (panels G-I). Both H and 4 also displayed scattered labeling of Purkinje cells and presumptive interneurons of the molecular layer. These neurons were most prominent in Line 4 using the Ai3 and R26R reporters. *Scale bar = 200 μm*

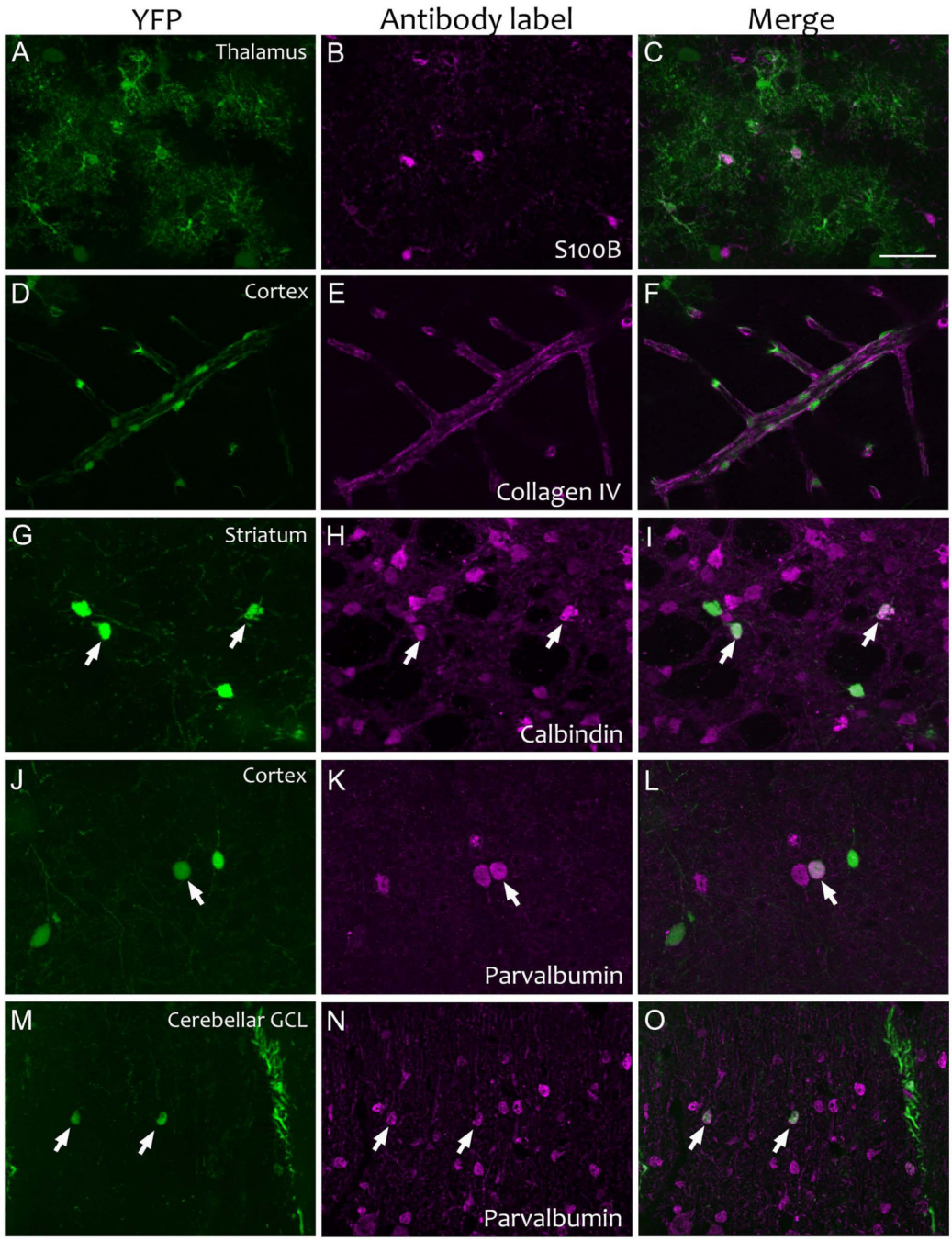

Figure 5. Cellular identity of ectopic YFP expression identified by immunofluorescent co-labeling for selective protein markers

Immunostains for S100B, collagen IV, calbindin, and parvalbumin were used to identify YFP-positive astrocytes in the thalamus (panels A-C), vascular endothelia and pericytes in the cortex (panels D-F), medium spiny neurons in the striatum (panels G-I), and GABAergic interneurons in the cortex (panels J-L) and cerebellum (panels M-O). The first panel in each row shows native YFP fluorescence (panels A, D, G, J, and M), the middle panel shows fluorescent immunostaining (panels B, E, H, K, and N), and the final panel shows a merge

of the two (panels C, F, I, L, and O). All tissue is from Line 4 × Ai3 animals treated with tamoxifen (collagen IV, parvalbumin) or vehicle (S100B, calbindin). *Scale bar = 40 μm*

Table 1

Antibodies used in this study

Antigen	Immunogen	Manufacturer details	Dilution
Calbindin D28k	Recombinant rat full-length protein	Swant (Marly, Switzerland) rabbit polyclonal, CB-38a	1:5000
Collagen IV	Collagen IV purified from human and cow placenta	Abcam (Cambridge, UK), rabbit polyclonal, ab6586	1:500
Green fluorescent protein (GFP)	Recombinant full-length protein	Abcam (Cambridge, UK), chicken polyclonal IgY, ab13970	1:1000
Nestin	Nestin purified from embryonic rat spinal cord	Millipore (Temecula, CA), mouse monoclonal IgG1, clone rat-401/MAB353	1:200
Parvalbumin	Parvalbumin purified from rat muscle	Swant (Marly, Switzerland) goat polyclonal, PVG-214	1:1000
S100B	S100 protein purified from cow brain	Dako (Carpinteria, CA) rabbit polyclonal IgG, Z0311	1:100

Table 2

Comparison of Cre reporter lines used in this study

Reporter line	Strain background	Targeting site	Promoter	Transcriptional stop size	Reporter	Sensitivity
Ai3	C57BL/6	ROSA26	CAG + ROSA26	0.9 kb	YFP (native fluorescence)	High
R26R	C57BL/6	ROSA26	ROSA26	2.7 kb	LacZ (enzymatic detection)	Medium
GluCl	C57BL/6	ROSA26	CAG + ROSA26	2.7 kb	YFP (antibody detection)	Low

Table 3

Estimated extent of ectopic labeling in nestin-CreER^{T2} × Ai3 offspring

	K × Ai3			H × Ai3			4 × Ai3		
Area	**Total**	**Neurons**	**Non-neuronal cells**	**Total**	**Neurons**	**Non-neuronal cells**	**Total**	**Neurons**	**Non-neuronal cells**
CA1	**0.24 ± 0.26 %**	0.09 ± 0.15 %	0.15 ± 0.14%	**52.0 ± 2.8 %**	51.7 ± 3.0 %	0.24 ± 0.21 %	**5.0 ± 0.5 %**	1.3 ± 0.8 %	3.7 ± 0.8 %
CA3	**0.15 ± 0.26 %**	0 %	0.15 ± 0.26 %	**22.1 ± 3.7 %**	19.7 ± 4.6 %	2.42 ± 1.97 %	**9.4 ± 5.2 %**	0.7 ± 0.6 %	8.7 ± 4.7 %
Cortical L2/3	**0.34 ± 0.16 %**	0.20 ± 0.08 %	0.14 ± 0.25 %	**3.6 ± 1.5 %**	1.3 ± 0.9 %	2.34 ± 0.89 %	**11.9 ± 3.5 %**	1.6 ± 0.3 %	10.3 ± 3.7 %
Cortical L5/6	**0.28 ± 0.14 %**	0.13 ± 0.13 %	0.15 ± 0.14 %	**24.7 ± 4.9 %**	23.0 ± 5.5 %	1.69 ± 0.60 %	**12.1 ± 1.5 %**	0.5 ± 0.2 %	11.6 ± 1.5 %

Table 4

Comparison of nestin-CreER^{T2} lines used in this study

Nestin-CreER^{T2} Line	Nestin sequence elements	Tamoxifen-independent expression in Ai3	Tamoxifen-induced expression in Ai3	Original reference
Line K	5.8 kb rat *nestin* promoter + 5.4 kb fragment including partial exons 1 and 4, entire exons 2 and 3, and intervening introns	Minor labeling of ventricular ependymal cells	Strong labeling of SVZ, moderate labeling of SGZ, rare astrocytes and neurons noted outside neurogenic zones	(Lagace et al., 2007)
Line H	5.4 kb rat *nestin* promoter + 0.65 kb of second intron in reverse orientation	Sparse labeling of astrocytes in thalamus and cortex, neurons in cerebellum, striatum	Strong labeling of SVZ, SGZ, cerebellar granule cells, pyramidal neurons in CA1, CA3, EC, and neocortical layer 5	(Dranovsky et al., 2011; Sahay et al., 2011a)
Line 4	5.8 kb rat *nestin* promoter + 1.8 kb spanning second intron	Moderate labeling of astrocytes in thalamus and cortex, neurons in cerebellum, striatum, cortex and hippocampus	Strong labeling of SVZ, SGZ, cerebellar granule cells, vascular endothelium and pericytes	(Imayoshi et al., 2006)